frontiers in Physics

REVIEW
published: 20 March 2019
doi: 10.3389/fphy.2019.00033

Double Beta Decay Experiments With Loaded Liquid Scintillator

Itaru Shimizu[1]* *and Mark Chen*[2]

[1] Research Center for Neutrino Science, Tohoku University, Sendai, Japan, [2] Department of Physics, Engineering Physics and Astronomy, Queen's University, Kingston, ON, Canada

Liquid scintillator detectors have many properties which are highly advantageous for neutrino research at the MeV energy scale. There are various choices of additives to an organic liquid scintillator which typically function as the nuclear targets in a neutrino interaction. More recently, new techniques for loading a large amount of nuclei into liquid scintillator enable sensitive searches for double beta decay with various nuclei. KamLAND was an existing detector constructed for neutrino physics at the MeV scale, later upgraded to a sensitive detector for double beta decay (KamLAND-Zen). In this experiment, isotopically enriched xenon gas was loaded into the highly radiopure liquid scintillator. As xenon is a stable noble gas, the scintillation performance changes little, and it is safe for long-term use. To mitigate backgrounds, xenon was loaded only into the liquid scintillator in the central part of the detector, contained in a spherical nylon balloon. Owing to the large amount of xenon and low background level, the KamLAND-Zen experiment achieved the most sensitive search to date for neutrinoless double beta decay in the standard mechanism. The next phase of the experiment plans to increase the amount of xenon by almost double. In the future, sensitivity can be further enhanced by detector upgrades. SNO+ (successor to the Sudbury Neutrino Observatory) is a liquid scintillator detector that is currently being commissioned and will soon be taking data. Originally, SNO+ developed a technique to load neodymium into the liquid scintillator in order to conduct a double beta decay search with the isotope ^{150}Nd. Later, SNO+ developed two new techniques that enable loading tellurium into liquid scintillator. The large natural abundance of ^{130}Te and the ability to load tellurium at a significant concentration in the SNO+ liquid scintillator, while maintaining excellent scintillation optical properties, offer the prospect of a very sensitive search for neutrinoless double beta decay. This article will discuss both experiments, KamLAND-Zen and SNO+, highlighting the results achieved, the techniques involved in loading the liquid scintillator, and describing the purification of components of the loaded liquid scintillator to very low background levels.

Keywords: loaded liquid scintillator, double beta decay, Majorana neutrinos, low energy neutrinos, radio-purification

OPEN ACCESS

Edited by:
Alexander S. Barabash, Institute for Theoretical and Experimental Physics, Russia

Reviewed by:
Hiroyasu Ejiri, Osaka University, Japan
Fedor Danevich, National Academy of Sciences of Ukraine (NAN Ukraine), Ukraine

***Correspondence:**
Itaru Shimizu
shimizu@awa.tohoku.ac.jp

Specialty section:
This article was submitted to High-Energy and Astroparticle Physics, a section of the journal Frontiers in Physics

Received: *19 December 2018*
Accepted: *22 February 2019*
Published: *20 March 2019*

Citation:
Shimizu I and Chen M (2019) Double Beta Decay Experiments With Loaded Liquid Scintillator. Front. Phys. 7:33. doi: 10.3389/fphy.2019.00033

1. INTRODUCTION

Liquid scintillator detectors have been an important tool in nuclear and particle physics since they were invented in the 1950's. Other research fields have also found uses for liquid scintillator. A liquid scintillator is an organic liquid that gives off light when excited by energetic particles and radiation. When the molecules of a scintillating medium de-excite, fluorescence light is emitted. The amount of fluorescence light that is collected and detected is used to infer the energy that was deposited by the particle interaction. Thus, spectroscopy or calorimetry is the typical application of a liquid scintillator; however, there have also been many instances of application of liquid scintillator detectors for timing, position and particle identification measurements.

A liquid scintillator detector has several advantages. A large detector can be constructed and easily filled, economically, with a liquid scintillating material; in contrast, fabricating a detector with solid scintillating material can be cumbersome and expensive (although there is the trade-off that a liquid requires containment, which can be non-trivial). A liquid scintillator is made from hydrocarbon compounds and thus has atomic constituents with low Z and A (atomic number and atomic mass, respectively). The time response of an organic liquid scintillator is typically very fast, with a decay time around a few nanoseconds. Liquid scintillators have good linearity of response; the light output does have some dependence, in a measurable way, on the type of particle that produced the ionization or energy deposit in the medium [1]. This latter property can be used to identify the type of particle that interacted in the medium. One particular advantage of a liquid scintillator that has recently been exploited is the fact that an organic liquid tends to have very low levels of radioactive background impurities. Naturally occurring radioactive backgrounds in experiments come from trace amounts of elements such as uranium, thorium and potassium. An organic liquid has very low levels of these contaminants due to the fact that ionic impurities (such as U, Th, and K) do not dissolve easily in a non-polar organic medium. Large scintillating detectors such as Borexino (and the Borexino Counting Test Facility) demonstrated in the 1990's that very low backgrounds can be achieved in a liquid scintillator detector [2].

As a consequence of several of these favorable properties, liquid scintillators have become very prominent today in the field of neutrino physics. Neutrino detection requires very large targets that have very low backgrounds. Liquid scintillators fit the bill. An organic liquid scintillator typically emits ∼10,000 photons/MeV of energy deposited. Not all of these photons are detected—far from it—nevertheless, detecting scintillation photons using photomultiplier tubes (PMTs) is relatively straightforward and it is clear that a large scintillation detector with sensitivity to events at the MeV level (or below) can be conceived of and then realized. In that vein, it was Raghavan [3] who proposed in 1994 that a large liquid scintillator detector could serve as the platform in which a sensitive double beta decay experiment could be deployed. Liquid scintillators can be loaded with isotopes (elements) that have the possibility to undergo double beta decay. One of the necessary requirements for a sensitive double beta decay experiment is very low backgrounds; this requirement, along with the large scale that can be realized with a liquid scintillator detector, suggests that double beta decay experiments with loaded liquid scintillator could be a very powerful approach in the search for this important neutrino physics signal.

2. SEARCH FOR NEUTRINOLESS DOUBLE BETA DECAY

In recent years neutrino oscillation experiments firmly established that neutrinos have flavor mixing and tiny masses, requiring modifications to the Standard Model of particle physics [4]. Thus, the origin of neutrino masses becomes one of the primary interests in particle physics. Unlike other charged fermions, the uncharged neutrino could be its own antiparticle, so-called Majorana neutrino proposed by Ettore Majorana. This hypothesis is important for constructing a theoretical mechanism to realize those tiny neutrino masses; however, there has been no experimental evidence for Majorana neutrinos so far. The practical way to probe the Majorana nature of neutrinos is the search for neutrinoless double beta decay ($0\nu\beta\beta$),

$$(A, Z) \rightarrow (A, Z+2) + 2e^{-} \tag{1}$$

which represents a rare nuclear decay emitting only two electrons without neutrinos, explicitly violating lepton number by two. If this reaction is mediated by the exchange of a light Majorana neutrino between two nucleons, its rate increases with the square of the effective Majorana neutrino mass $\langle m_{\beta\beta} \rangle \equiv \left| \Sigma_i U_{ei}^2 m_{\nu_i} \right|$, where U_{ei} is the 3×3 unitary neutrino mixing matrix, and m_{ν_i} are the masses of three neutrinos. Therefore, its measurement would provide information on the absolute neutrino mass scale and ordering. The Majorana neutrino hypothesis is theoretically favored because the right-handed heavy neutrino with masses at the GUT scale naturally leads to the light neutrino masses (see-Saw mechanism). In addition, the CP violating decay of the heavy neutrino in the early Universe could explain the matter dominance in the universe (Leptogenesis). Majorana neutrinos are a key piece in particle physics and cosmology, and the determination of its related parameters such as Majorana neutrino masses and CP phases is of critical importance.

Other observations in neutrino oscillations and cosmology related to neutrino masses provide good milestones of the $0\nu\beta\beta$ search. There are two possibilities of the mass ordering in the three neutrinos, the normal mass hierarchy (NH) with one heavier neutrino relative to the other two, or the inverted mass hierarchy (IH) with two heavier neutrinos; the mass hierarchy gives rise to different $\langle m_{\beta\beta} \rangle$ depending on the absolute scale of the three neutrino masses. In general, order 1 ton of $\beta\beta$ isotope is required to have $\langle m_{\beta\beta} \rangle$ sensitivity down to 10−20 meV. The sensitivity that an experiment can reach depends on the background levels that are achieved in a given experiment, as well as the nuclear matrix element and phase space factor for the chosen isotope. There is also a general dependence on g_A, the strength of the axial coupling constant and whether it is quenched or not. To probe down to a few meV corresponding to the NH region, experiments will need to increase their exposures by at

least one order of magnitude as a general requirement, which assumes background levels are the same. If backgrounds increase with added $\beta\beta$ isotope mass, the required exposure would need to be even greater, requiring many tons of isotope. Most of the near-future experiments aim to investigate the IH region. On the other hand, cosmological surveys have sensitivity to the sum of the three neutrino masses (Σm_ν). A positive value of Σm_ν from future cosmology observations would provide another milestone. If a positive $0\nu\beta\beta$ signal is found with the rate expected from other observations, the scenario of the light Majorana neutrino exchange can be proved. Even if negative, the contradiction with other observations disproves the standard scenario, potentially resulting in a big impact on particle physics and cosmology.

The isotopes commonly used for the study of double beta decay are listed in **Table 1**. There are no isotope specially favored in the $0\nu\beta\beta$ half-life predicted from the phase space factor and nuclear matrix element (NME), however, there are several favored isotopes for practical reasons. The theoretical estimates on NMEs highly depend on the many-body approaches used for their calculations, in addition, the possible quenching of the axial-vector coupling can reduce NMEs, resulting in the significant reduction of the experimental $\langle m_{\beta\beta}\rangle$ sensitivity [18]. In general, isotopic enrichment is essential to enhance the $0\nu\beta\beta$ search sensitivity. The only exception is ^{130}Te with the large natural abundance (34.2%), providing a great advantage in lowering costs. Although the natural abundance of ^{136}Xe is only 8.9%, its isotopic enrichment is easier and relatively low-cost owing to the characteristics of gases allowing centrifugation for the mass production of isotopes. In contrast to those isotopes, the production of ^{76}Ge is relatively high-cost; however, it is highly desirable since pure germanium is a semiconductor and can function as a detector with high energy resolution. Among these isotopes, the natural abundance in ^{48}Ca is the lowest (0.19%); however, the Q-value is the highest, and this is most advantageous for reducing radioactive backgrounds.

The history of double beta decay research is briefly reviewed below. In 1939, Furry suggested the idea of the $0\nu\beta\beta$ for the first time [19]. The $0\nu\beta\beta$ process requires the virtual intermediate state of a nucleus in the same manner as the $2\nu\beta\beta$ process introduced by Goeppert-Mayer, and also a Majorana neutrino. The first experimental search was performed by Fireman in 1948 using Geiger counters and 25 g of enriched ^{124}Sn [20]. The following experiments used various particle detectors, such as Geiger, proportional, and scintillation counters, and so on. The initial $0\nu\beta\beta$ experiments often found positive signals, however later experiments disprove them. After the discovery that the weak interaction violates parity conservation maximally in 1957, the $0\nu\beta\beta$ search was noted to be a challenging task due to a strong helicity suppression. The experiments using a semiconductor Ge detector (7.2 kg of natural Ge) reached a half-life sensitivity of higher than 10^{24} yr for ^{76}Ge in 1987 [21]. Further developing these detectors, IGEX (6.5 kg of enriched ^{76}Ge) and Heidelberg-Moscow (11 kg of enriched ^{76}Ge) experiments with enriched ^{76}Ge obtained limits of greater than 10^{25} yr for the half-life of the decay [22, 23]. In 2001, a part of the Heidelberg-Moscow collaboration claimed detection of $0\nu\beta\beta$ decay [24]. This claim was eagerly discussed and scrutinized, but remained uncertain. Independent tests were expected; however, searches with $\beta\beta$ nuclei other than ^{76}Ge did not yet have enough sensitivity to test this claim. The superiority of the $0\nu\beta\beta$ search in Ge was mainly due to the good energy resolution, which was difficult to achieve with other detectors.

Many experiments which have the ability to test the detection claim in ^{76}Ge with the sensitivity of $\sim$10$-$100 meV in $\langle m_{\beta\beta}\rangle$ were planned in the 2000's, and some of them have been launched. Various ideas have been considered to realize high sensitivity searches, utilizing new detector technologies and low background techniques developed in double beta decay, neutrino, and dark matter search experiments. Calorimeter experiments, i.e., experiments whose $\beta\beta$ source and detector are identical, are EXO, KamLAND-Zen, GERDA, MAJORANA, CUORE, CUPID, SNO+, NEXT, PandaX-III, etc. SuperNEMO is an external source experiment. An external source needs to be thin enough to allow electrons from $\beta\beta$ decays to escape without significant energy loss; hence it is not so easy to increase the source target mass compared to calorimeter experiments. If the $0\nu\beta\beta$ is discovered in the future, an external source experiment could provide an excellent measurement of the angular correlations and energies of the two emitted electrons; this would provide essential information to distinguish between different underlying mechanisms for the $0\nu\beta\beta$.

EXO-200 was launched in 2011 using a liquid xenon time projection chamber (TPC), containing $\sim$175 kg of xenon enriched to 80.6% in ^{136}Xe [25]. KamLAND-Zen was also launched in 2011 using a xenon-loaded liquid scintillator (LS) detector, containing 330 kg of xenon enriched to 90.9% in ^{136}Xe [26], later increasing the xenon amount. GERDA Phase I took data between 2011 and 2013 using coaxial detectors, containing 17.7 kg of germanium enriched to 86% in ^{76}Ge, and moved into the upgraded experiment GERDA Phase II in 2015 using BEGe detectors (20.0 kg of germanium) and coaxial detectors (15.6 kg of germanium) [27]. KamLAND-Zen and EXO-200 refuted the detection claim in ^{76}Ge considering available NME calculations [28], and GERDA Phase I refuted the claim in a model-independent way [27]. CUORE was launched in 2017 using a cryogenic bolometer array, containing 741 kg of TeO_2 with natural tellurium of which abundance in ^{130}Te is 34.2% [29]. SNO+ is a LS detector that is currently being commissioned and will load tellurium into the LS. The $0\nu\beta\beta$ search experiments are in intense competition for the first detection. Among them, the LS experiments have great advantages in reducing radioactive background and having scalability of isotope amount by enlarging the detector for future multi-purpose neutrino experiments. In this article, we focus on the LS experiments, KamLAND-Zen and SNO+, highlighting the results achieved, the techniques involved in loading the LS, and describing the purification of components of the loaded LS to very low background levels.

3. STATUS OF LOADED LIQUID SCINTILLATOR EXPERIMENTS

3.1. KamLAND-Zen

The Kamioka Liquid scintillator Anti-Neutrino Detector (KamLAND) was built and started operation in 2002 primarily

TABLE 1 | Predicted $T^{0\nu}_{1/2}$ at $\langle m_{\beta\beta}\rangle = 50$ meV from Rodin et al. [5] ([6] for ^{48}Ca), measured $T^{2\nu}_{1/2}$, natural abundance [7], Q-value [8] for commonly used isotopes.

Isotope	$T^{0\nu}_{1/2}$ @ 50 meV (yr)	$T^{2\nu}_{1/2}$ measured (yr)	Natural abundance (%)	Q-value (keV)
^{48}Ca	4.32×10^{27}	$(6.4\,^{+0.7}_{-0.6}\,^{+1.2}_{-0.9}) \times 10^{19}$ [9]	0.19	4,268
^{76}Ge	0.86×10^{27}	$(1.926 \pm 0.094) \times 10^{21}$ [10]	7.8	2,039
^{82}Se	2.44×10^{26}	$(9.39 \pm 0.17 \pm 0.58) \times 10^{19}$ [11]	8.8	2,998
^{96}Zr	0.98×10^{27}	$(2.35 \pm 0.14 \pm 0.16) \times 10^{19}$ [12]	2.8	3,356
^{100}Mo	2.37×10^{26}	$(7.11 \pm 0.02 \pm 0.54) \times 10^{18}$ [13]	9.7	3,034
^{116}Cd	2.86×10^{26}	$(2.630 \pm 0.011\,^{+0.113}_{-0.123}) \times 10^{19}$ [14]	7.5	2,813
^{130}Te	2.16×10^{26}	$(0.82 \pm 0.02 \pm 0.06) \times 10^{21}$ [15]	34.1	2,528
^{136}Xe	4.55×10^{26}	$(2.165 \pm 0.016 \pm 0.059) \times 10^{21}$ [16]	8.9	2,458
^{150}Nd	2.23×10^{25}	$(9.34 \pm 0.22\,^{+0.62}_{-0.60}) \times 10^{18}$ [17]	5.6	3,371

to search for the oscillation of anti-neutrinos emitted from distant nuclear power reactors, typically at 180 km. It has presented an evidence of anti-neutrino disappearance, and solved the long-standing solar neutrino problem [30]. Its precise measurement has also demonstrated two cycles of the clear oscillatory behavior in the survival probability [31]. The new knowledge of how anti-neutrinos propagate allows KamLAND to estimate radiogenic heat via the observation of the geologically produced anti-neutrinos (geo neutrinos) from ^{238}U and ^{232}Th [32, 33]. Those achievements are owing to the huge and highly radiopure LS suited to the rare event search.

The idea of loading xenon into LS was firstly discussed in Raghavan [3]. Xenon is soluble in the LS up to a few percent, by weight. The heavy isotope ^{136}Xe with natural abundance of 8.9% is a $\beta\beta$ nucleus with the Q-value of 2.458 MeV. The two coincident electrons from $\beta\beta$ decay produce simultaneous scintillation light, so only their summed energy is observed by a detector. The sum is the Q-value for $0\nu\beta\beta$ decays. For $2\nu\beta\beta$ decays the sum has a continuous spectrum up to the Q-value, which introduces a background for the $0\nu\beta\beta$ search due to the limited energy resolution. The well-known 2.614 MeV γ-rays from ^{208}Tl of a ^{232}Th daughter nucleus is not a serious background for the $0\nu\beta\beta$ search if the coincident β/γ are detected in homogeneous active detectors. Unlike heterogeneous detectors, e.g., Ge detectors, backgrounds from natural radioactivities are extremely small, so the primary background source for an underground LS detector will be muon spallation products and solar neutrinos. However, it is necessary to enrich xenon in ^{136}Xe and to hold the xenon loaded LS (Xe-LS) in a clean container for realizing a sensitive $0\nu\beta\beta$ search [34]. KamLAND-Zen (KamLAND Zero-Neutrino Double-Beta Decay) project has been launched in 2009 to aim for the realization of the above concept.

The construction of the KamLAND-Zen detector illustrated schematically in **Figure 1** was done in the summer of 2011. The $\beta\beta$ decay source, 320 kg of enriched xenon dissolved into the LS, was contained in a 3.08-m-diameter spherical inner balloon (IB) at the center of the detector. The IB is surrounded by 1 kton of LS (Outer-LS) contained in a 13-m-diameter spherical outer balloon (OB) made of 135-μm-thick nylon/EVOH composite film. The Outer-LS acts as the huge and ultra-clean (^{238}U: 3.5×10^{-18} g/g, ^{232}Th: 5.2×10^{-17} g/g) active shield, so the external γ-ray backgrounds are negligible. Buffer oil (BO) between the OB and an 18-m-diameter spherical stainless-steel containment vessel (SST) shields the LS from external γ-rays. The scintillation photons from the LS are viewed by 1,325 17-inch and 554 20-inch photomultiplier tubes (PMTs) mounted on the inner surface of the SST, providing 34% solid-angle coverage. The Xe-LS consists of 82% decane and 18% pseudocumene (1,2,4-trimethylbenzene) by volume, 2.7 g/L of the fluor PPO (2,5-diphenyloxazole), and (2.44 ± 0.01)% by weight of enriched xenon gas. The isotopic abundances in the enriched xenon were measured by a residual gas analyzer to be (90.93 ± 0.05)% ^{136}Xe, (8.89 ± 0.01)% ^{134}Xe.

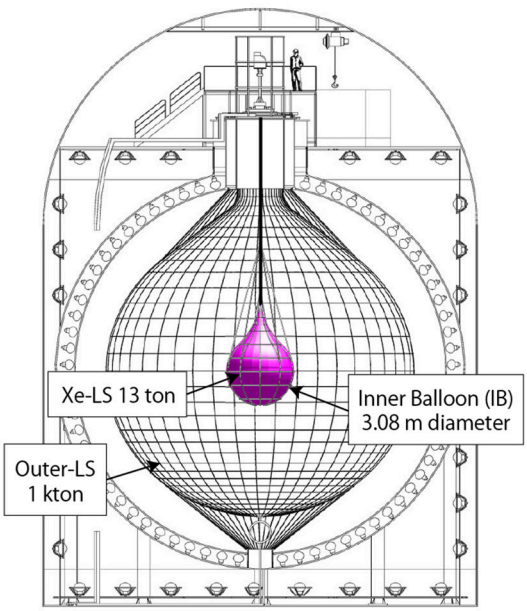

FIGURE 1 | Schematic diagram of the KamLAND-Zen detector. The Xe-LS (13 ton) is contained in a 3.08-m-diameter spherical inner balloon (IB), surrounded by 1 kton of the LS (Outer-LS).

The requirement for radioactive contaminants in the IB is rather tight for ^{238}U because its daughter nucleus ^{214}Bi ($\beta + \gamma$)

is a background source for the $0\nu\beta\beta$ search. The IB is made from 25-μm-thick transparent Nylon-6 film specially produced without reinforcing filler, which was identified as the main source of radioactive contaminants. Its mechanical strength is 19.4 N/m, and xenon permeability from total surface area is <220 g/year. The measured contaminants of the film by ICP-MS was 1.5×10^{-10} g/g for ^{238}U and 5.9×10^{-11} g/g for ^{232}Th. After ultrasonic cleaning of the film in pure water, the contaminants were reduced to 2×10^{-12} g/g for ^{238}U and 3×10^{-12} g/g for ^{232}Th, indicating removal of attached dust on the film. So this cleaned film was selected as the IB material, and all the production process has been done in a super cleanroom with Class 1 (<1 particle at 0.5 μm or larger per cubic feet) in Tohoku University. To avoid dust attachment, the film has been handled with wearing rubber gloves and a clean suit, and operating neutralization apparatus. The water-dropped shape balloon was constructed by fixing 24 gores (sectors of curved surface between two close longitude lines) with a specially developed heat welding method. The leaks along the welding lines were stringently checked by He leak test, and a small piece of film (patch film) was attached on each leak point with an adhesive. The completed IB was trucked to the KamLAND site in the Kamioka mine. It was sunk into the KamLAND detector through a narrow hole at the top in a cleanroom with Class 10−100. Finally, the IB was inflated with the LS without xenon and then replaced with Xe-LS. It is suspended by 12 film straps of the same material. An initial $0\nu\beta\beta$ decay search with high sensitivity was quickly realized, owing to the extremely low radioacitivity in the already existing KamLAND detector, and the minimization of additional radioactivities achieved in the manufacturing of the IB.

KamLAND-Zen presented results of the first phase of the science run (phase I) collected between October 12, 2011 and June 14, 2012 [28]. The data acquisition system (DAQ) is triggered when the 17-inch PMT hits are 70 or more (primary trigger), corresponding to an energy threshold of ∼0.4 MeV. After primary trigger events, the threshold is lowered to ∼0.25 MeV for 1 ms to study sequential decays of Bi-Po in the ^{238}U or ^{232}Th daughters. Event energy (visible energy) is estimated from the number of photo-electrons (p.e.) after corrections on the light collection efficiency which depends on the event vertex. The vertex is reconstructed with the PMT hit-time distribution after subtracting the photons' time of flight. Energy calibration is performed using ^{214}Bi β's and γ's from ^{222}Rn ($\tau = 5.5$ day) introduced during the Xe-LS filling, ^{208}Tl 2.615 MeV γ's from a ThO_2W source deployed on the surface of the IB, and 2.225 MeV γ's from neutron captures on protons. Uncertainties from the non-linear energy response due to the quenching of the Xe-LS scintillation and Cherenkov light contributions are constrained by those calibrations. The neutron capture γ data indicates that the energy scale is stable within 1.0% over the volume and data-taking period. The vertex resolution is $\sigma \sim 15\,\mathrm{cm}/\sqrt{E(\mathrm{MeV})}$, and the energy resolution is $\sigma = (6.6 \pm 0.3)\%/\sqrt{E(\mathrm{MeV})}$.

The data just after the start of the KamLAND-Zen data-taking showed that the Xe-LS and IB are contaminated by unexpected background sources. Unlike the Outer-LS data which had been taken so far, the observed energy spectra did not agree with the expectations from natural radioactivities or muon spallation products. What stood out were several unidentified peaks with their vertices at the IB, and more importantly, a peak around 2.6 MeV overlapping with the $0\nu\beta\beta$ search window. Possible background sources for those peaks, which may have been introduced due to the installation activities, or due to muon spallation on xenon, were investigated. The background sources for lower energy peaks at the IB were identified as ^{134}Cs ($\beta + \gamma$) and ^{137}Cs (0.662 MeV γ). The observed ratio of ^{134}Cs/^{137}Cs activities on the IB was ∼0.8, which is consistent with contamination by radioactive fallout from the Fukushima-I reactor accident in March 2011. It was supposed that the contamination was caused by the attachment of the fallout on the film during construction, because the IB production facility was located just 100 km away from the Fukushima-I reactor site, and the Cs activities in a soil sample around the facility are comparable to natural radioactivities. For the background identification in the $0\nu\beta\beta$ window, all nuclei and decay schemes in the ENSDF database (containing basic data related to nuclear structure and decays) have been surveyed by the calculation of visible energy spectra with unstable isotopes considering the sequential decay and pile-up in the DAQ event window, and the non-linear energy response to all individual decay secondaries for each branch. Potential background sources for a peak around 2.6 MeV were identified as ^{110m}Ag (β^- decay, $\tau = 360$ day, $Q = 3.01$ MeV), ^{88}Y (EC decay, $\tau = 154$ day, $Q = 3.62$ MeV), ^{208}Bi (EC decay, $\tau = 5.31 \times 10^5$ yr, $Q = 2.88$ MeV), and ^{60}Co (β^- decay, $\tau = 7.61$ yr, $Q = 2.82$ MeV), based on the isotope survey with decay parent lifetimes longer than 30 days.

Figure 2 shows the observed energy spectrum and event rate variation for $2.2 < E < 3.0$ MeV based on the full data-set with an exposure of 89.5 kg-yr of ^{136}Xe. It indicates that the background source in the $0\nu\beta\beta$ search is dominated by the ^{110m}Ag contribution. The possibility of the ^{110m}Ag contamination had been carefully investigated considering all the *in-situ* and *ex-situ* measurements for radioactivities of the detector material. Observation of ^{134}Cs/^{137}Cs on the IB indicates the ^{110m}Ag contamination by Fukushima fallout, because ^{110m}Ag is also detected in a soil sample around the production facility. The ^{110m}Ag activity is two orders of magnitude less than ^{137}Cs. However, if the ratio of ^{110m}Ag/^{137}Cs activities for the IB and soil is constant, the amount of ^{110m}Ag from Fukushima fallout is enough to explain the observed rate for a peak around 2.6 MeV. Another possibility of the ^{110m}Ag contamination is cosmogenic production by xenon spallation. In general, the cosmogenic activation of detector materials above ground will cause long-lived nuclei which survive until the start of experiments underground, resulting in background sources in the $0\nu\beta\beta$ search. The cross section of the ^{136}Xe spallation was measured with accelerated ^{136}Xe beam equivalent with 1 GeV protons incident on ^{136}Xe [35]. Geant4 simulation, which reproduces these production rates for order estimation, indicates ^{88}Y and ^{110}Ag from the ^{136}Xe spallation become dominant background sources in the $0\nu\beta\beta$ search after a few 100 days of storage. The expected rates are enough to explain the observed rate; however, their transport efficiencies into the Xe-LS is difficult to know.

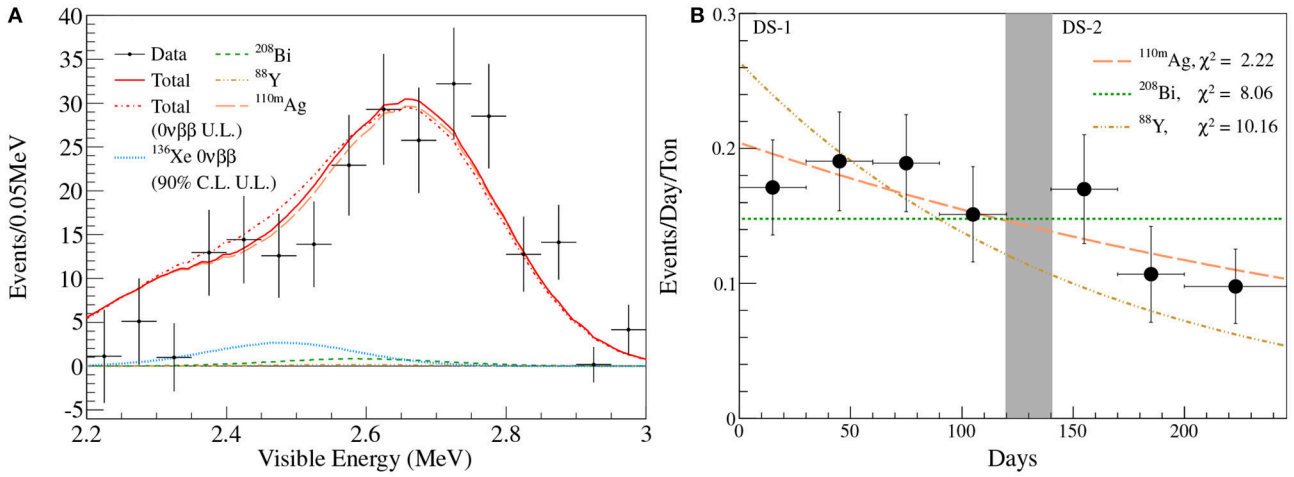

FIGURE 2 | (A) Energy spectrum of selected candidate events together with best-fit backgrounds and **(B)** event rate variation for $2.2 < E < 3.0$ MeV after subtracting known background contributions. Figures are adopted from [28].

Even for the unexpected background contaminations mentioned above, the KamLAND-Zen data provided various remarkable results in the $\beta\beta$ research. A fiducial volume cut to suppress the backgrounds on the IB showed a clear signal from $2\nu\beta\beta$ decays with high statistics. The measured $2\nu\beta\beta$ half-life of ^{136}Xe is $T^{2\nu}_{1/2} = 2.30 \pm 0.02(\text{stat}) \pm 0.12(\text{syst}) \times 10^{21}$ yr [36], which is consistent with the result obtained by EXO-200, $T^{2\nu}_{1/2} = 2.11 \pm 0.04(\text{stat}) \pm 0.21(\text{syst}) \times 10^{21}$ yr [25]. The measured $T^{2\nu}_{1/2}$ is significantly lower than the lower limit in [37, 38]. In the $0\nu\beta\beta$ search window, the background is dominated by ^{110m}Ag decays in the Xe-LS. The 90% C.L. lower limit on the $0\nu\beta\beta$ half-life is $T^{0\nu}_{1/2} > 1.9 \times 10^{25}$ yr [28]. The hypothesis that backgrounds from ^{88}Y, ^{208}Bi, and ^{60}Co are absent marginally increases the limit to $T^{0\nu}_{1/2} > 2.0 \times 10^{25}$ yr (90% C.L.). A combined limit from KamLAND-Zen and EXO-200 [39] gives $T^{0\nu}_{1/2} > 3.4 \times 10^{25}$ yr (90% C.L.), corresponding to a 90% C.L. upper limit on the effective Majorana neutrino mass, $\langle m_{\beta\beta} \rangle < (120 - 250)$ meV considering available NME calculations [6, 40–42]. The combined result for ^{136}Xe refutes the $0\nu\beta\beta$ detection claim in ^{76}Ge [43] at >97.5% C.L. for the considered NME calculations [28].

KamLAND-Zen also searched for some exotic decay modes. In particular, a lower limit on the ordinary Majoron-emitting decay half-life of ^{136}Xe is obtained as $T^{0\nu\chi^0}_{1/2} > 2.6 \times 10^{24}$ yr at 90% C.L., which is a factor of five more stringent than previous limits [37]. The limit on single-Majoron emission can be translated into a limit on the effective coupling constant of the Majoron to the neutrino, $\langle g_{ee} \rangle$ [44], using the relation,

$$T^{-1}_{1/2} = \left| \langle g_{ee} \rangle \right|^2 |M|^2 G \quad \text{for } 0\nu\beta\beta\chi^0 . \tag{2}$$

then an upper limit of $\langle g_{ee} \rangle < (0.8 - 1.6) \times 10^{-5}$ at 90% C.L. is obtained [36]. Combining a limit obtained by the neutrino data from SN1987A significantly extends the limit down to $\langle g_{ee} \rangle < 4 \times 10^{-7}$. This limit excludes the possibility that ordinary Majoron-emitting decay modes play a dominant role to light Majorana neutrino exchange for $\langle m_{\beta\beta} \rangle > 20$ meV.

The sensitivity of the $0\nu\beta\beta$ search in the phase I data was limited by the background peak around 2.6 MeV from ^{110m}Ag decays. To achieve the designed sensitivity in KamLAND-Zen, the collaboration embarked on a purification campaign to reduce ^{110m}Ag by a significant factor as illustrated in **Figure 3**. At the beginning of the campaign, xenon was extracted from the detector by LS circulation, whose intake and outtake were near the bottom and top of the IB volume, followed by degassing in a buffer tank in June 2012. To keep a high xenon extraction efficiency, the LS mixing within the IB volume was minimized through strict density and temperature control. The data taken for about 1 month after the xenon extraction showed that ^{110m}Ag remained in the Xe-depleted-LS as expected. It has demonstrated that On/Off (Xe-LS/Xe-depleted-LS) measurements to cross-check the estimated background rate are possible in KamLAND-Zen. In the future, if a positive signal is observed, such measurements will be a powerful tool to claim the $0\nu\beta\beta$ detection. The extracted xenon and additional new xenon were purified by distillation and refined with a heated zirconium getter. The Xe-depleted-LS was replaced by the new LS, purified by water extraction and vacuum distillation. Although a significant reduction of ^{110m}Ag was expected, the reduction was only a factor of 3-4, possibly due to ^{110m}Ag release from the IB film or partial LS mixing during filling. To achieve the reduction goal, the LS purification was performed by three volume exchanges in circulation mode. Finally, the xenon was dissolved again into the new purified LS in November 2013.

The second science run (phase II) started in December 2013 showed a reduction of ^{110m}Ag by more than a factor of 10. KamLAND-Zen reported on the analysis of the complete phase II data-set, collected between December 11, 2013 and October 27, 2015 [45]. In phase II, the xenon concentration in the LS, which consisted of 81% decane and 19% pseudocumene (1,2,4-trimethylbenzene) by volume, 2.29 g/L of the fluor PPO (2,5-diphenyloxazole), was increased to (2.91 ± 0.04)%. The isotopic

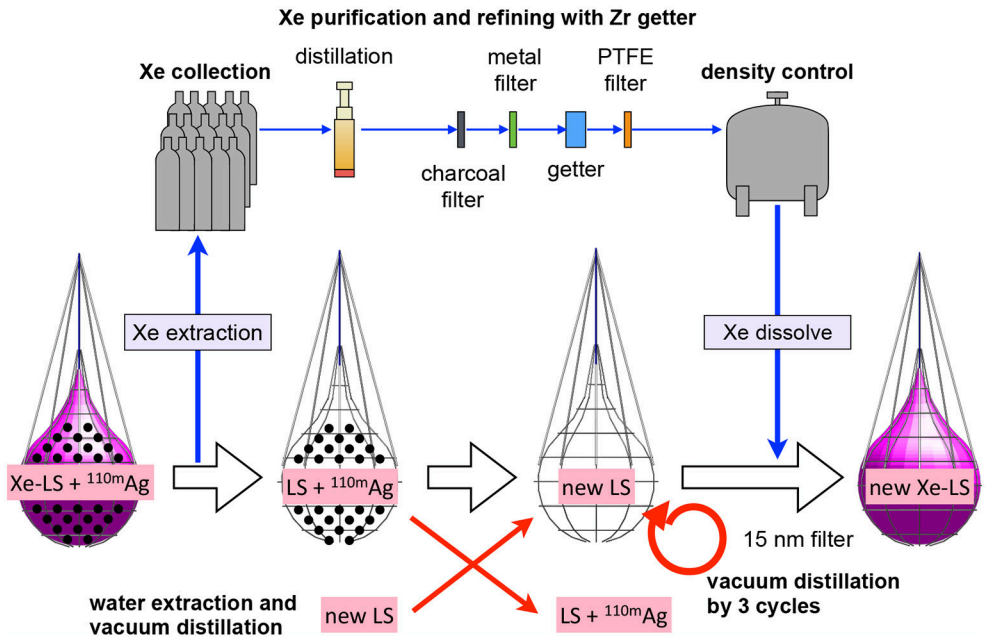

FIGURE 3 | Strategy of the Xe-LS purification to reduce ^{110m}Ag. After the xenon extraction, the ^{110m}Ag containing LS was replaced by the new purified LS. The extracted xenon was purified and dissolved into the LS again.

abundances in the enriched xenon were (90.77 ± 0.08)% ^{136}Xe, (8.96 ± 0.02)% ^{134}Xe. The total livetime was 534.5 days, which corresponds to an exposure of 504 kg-yr of ^{136}Xe with the whole Xe-LS volume.

Following the end of phase-II data-taking, the KamLAND-Zen detector calibration was performed using radioactive sources deployed at various positions along the central axis of the IB. In KamLAND, a new ultra-clean source deployment system, named as "MiniCal" due to its compact size, had been developed to avoid contaminating the LS for the ^{7}Be solar neutrino observation [46]. It was reused also for the KamLAND-Zen calibration after several modifications necessary for the source deployment into the Xe-LS volume. Unlike for KamLAND calibration, the source needs to pass through a narrow straight tube 10 cm in diameter. For the IB safety, a soft Vectran cable to suspend the smoothly shaped weight and source was used to minimize the risk of nylon film damage. A stepper motor to turn a spool of cable was replaced with a manual hand crank (originally prepared for emergency operation of MiniCal) for a sensitive control of the cable tension during source deployment. Each deployment position was determined according to the cable marks (39 points) monitored with an infrared camera inside of the MiniCal box. The relative position accuracy of the source deployment was ∼1 mm. For efficient calibrations, a composite source containing ^{137}Cs, ^{68}Ge, and ^{60}Co was prepared with similar intensities. Before and during the deployment, the MiniCal box was continuously purged by pure nitrogen gas to prevent radon contamination. The deployment of the source through the straight nylon tube was viewed by a monitor camera at ∼70 cm away. For each source position, more than 10,000 events were recorded for each gamma source with a hit threshold of 50, lowered once per second for a duration of 100 ms. **Figure 4** shows the deviation of the positions and energies, indicating that the reconstruction reproduces the known source positions to <2.0 cm (<1.0 cm for events occurring within 1 m from the IB center), and the reconstructed energy varies <1.0%. The observed energy resolution was $\sigma \sim 7.3\%/\sqrt{E(\mathrm{MeV})}$, slightly worse relative to phase I due to an increased number of dead PMTs.

In the phase II data, the clear peak around 2.6 MeV from ^{110m}Ag decays disappeared; the primary backgrounds for the $0\nu\beta\beta$ decay search were ^{214}Bi (daughter of ^{238}U) on the IB, the ^{10}C muon spallation product, and a small contribution from remaining ^{110m}Ag. It was found that the ^{214}Bi background on the IB is radially attenuated but larger in the lower hemisphere. The analysis with a smaller fiducial volume is advantageous for less background, and disadvantageous for less exposure of ^{136}Xe. To optimize the analysis, a multi-volume selection was introduced, dividing the 2-m-radius fiducial volume into 20 equal-volume bins for each of the upper and lower hemispheres. It allows a simultaneous fit to the energy spectra for all volume bins. In the phase II data analysis, additional event selection criteria to reject spallation backgrounds were newly introduced. The dead-time free electronics (MoGURA) was incorporated in the KamLAND DAQ system in 2010, and the special trigger to take post-muon neutron events has been working since August 2012. For the ^{10}C rejection, spherical volume cuts ($\Delta R <$ 1.6 m) around the reconstructed neutron vertices were applied for 180 s. The deadtime introduced by all the spallation cuts is only 7%.

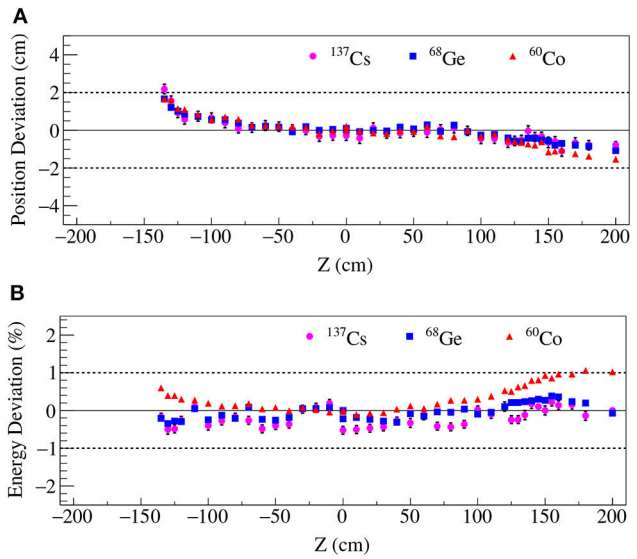

FIGURE 4 | (A) Deviation of the reconstructed position with respect to the true position and **(B)** deviation of the reconstructed energy with respect to $Z = 0$ cm for gamma calibration sources inside the IB.

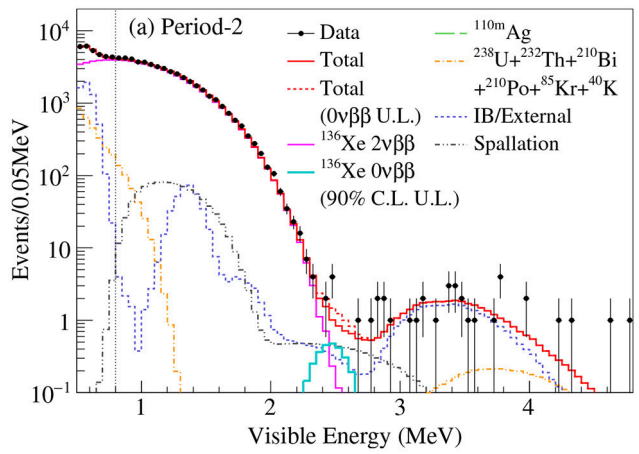

FIGURE 5 | Energy spectrum of selected $\beta\beta$ candidates within a 1-m-radius spherical volume in period 2 together with the best-fit backgrounds, the $2\nu\beta\beta$ decay, and the 90% C.L. upper limit for $0\nu\beta\beta$ decay. Figure is adopted from Gando et al. [45].

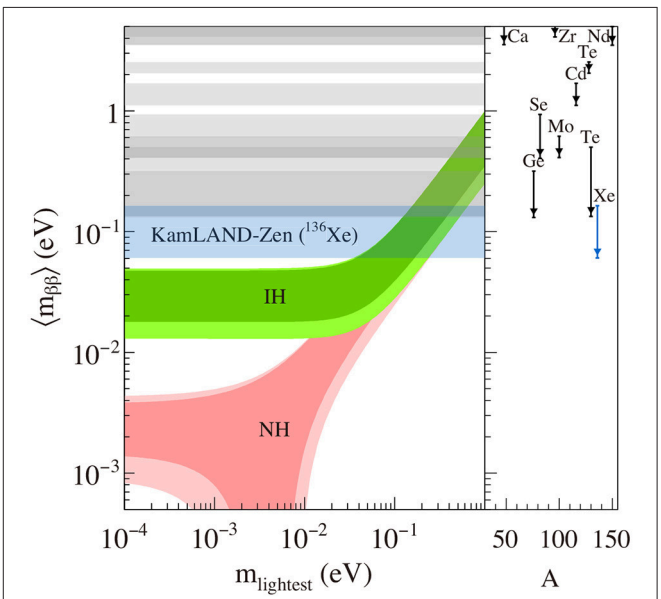

FIGURE 6 | Predictions on effective Majorana neutrino mass $\langle m_{\beta\beta}\rangle$ as a function of the lightest neutrino mass m_{lightest}, and the experimental limits from the $0\nu\beta\beta$ decay searches. Figure is adopted from Gando et al. [45]. The limits are recalculated from the updated half-life limits for ^{76}Ge [54], ^{82}Se [55], ^{116}Cd [14], and ^{130}Te [29].

The phase II data-set is divided into two equal time periods (period 1 and period 2) considering the possibility of the ^{110m}Ag decay. In the phase II data, the observed reduction of ^{110m}Ag is faster than the expectation from the lifetime, possibly due to dust settling to the bottom of the IB. There is no event excess over the background expectation for both data-sets. The low background levels achieved after the Xe-LS purification is highlighted by the observed energy spectrum within a 1-m-radius in period 2, as shown in **Figure 5**. The 90% C.L. lower limit on the ^{136}Xe $0\nu\beta\beta$ half-life is $T^{0\nu}_{1/2} > 9.2 \times 10^{25}$ yr. The combined limit with the phase I and phase II data is $T^{0\nu}_{1/2} > 1.07 \times 10^{26}$ yr (90% C.L.). The corresponding 90% C.L. upper limits on the effective Majorana neutrino mass $\langle m_{\beta\beta}\rangle$ are in the range $61 - 165$ meV using an improved phase space factor calculation [47, 48] and commonly used NME calculations [6, 40, 49–53] assuming the axial-vector coupling constant for the free nucleon value ($g_A \sim 1.27$). **Figure 6** shows the predictions on $\langle m_{\beta\beta}\rangle$ from neutrino oscillation parameters [56, 57] as a function of the lightest neutrino mass m_{lightest}, together with the experimental limits from the $0\nu\beta\beta$ decay searches for each nucleus [27, 58–60]. The upper limit on $\langle m_{\beta\beta}\rangle$ from KamLAND-Zen also provides the strongest constraint of $m_{\text{lightest}} < (180 - 480)$ meV (90% C.L.). In phase II, KamLAND-Zen have demonstrated effective background reduction in the xenon-loaded LS by purification, and improved the $0\nu\beta\beta$ search sensitivity.

3.2. SNO+

The Sudbury Neutrino Observatory (SNO) was a solar neutrino detector that took data from 1999 to 2006. SNO was a heavy water Cherenkov detector and it detected ^{8}B solar neutrinos using charged-current and neutral-current neutrino-deuteron reactions (as well as neutrino-electron elastic scattering). The comparison of signals from the different neutrino interactions in SNO proved that solar neutrinos, produced as electron-flavor neutrinos, are converted to other active flavors (i.e., muon and tau neutrinos) [61]. This discovery was awarded the 2015 Nobel Prize in Physics.

Near the end of the SNO experiment, plans were being formulated for a successor project. The heavy water in SNO was removed and returned to Atomic Energy of Canada Limited.

Most of the remaining SNO detector infrastructure was still in excellent condition making it possible to consider new experiments and future measurements. SNO+ was proposed and developed – the concept was to fill the SNO detector with liquid scintillator after the heavy water is removed. The physics capabilities of the SNO+ experiment were developed further and project funding was obtained in 2010. As a large detector to be filled with low background liquid scintillator, SNO+ has a broad range of neutrino physics topics that it can study. One of the prime objectives of SNO+ is the search for neutrinoless double beta decay.

Research for SNO+ double beta decay initially focused on the element neodymium. The isotope ^{150}Nd has the largest phase space of any of the candidate double beta decay isotopes; it also has the second highest *Q*-value. This was an interesting isotope to pursue since other large scale double beta decay experiments were focusing on Ge, Te, and Xe; therefore, developing the capability to deploy a large amount of neodymium would be complementary. Neodymium is a rare-earth lanthanide; another rare-earth element that is commonly loaded into liquid scintillator is gadolinium. Reactor neutrino experiments use gadolinium-loaded liquid scintillator to take advantage of the high neutron-capture cross section of Gd. SNO+ initially set out to produce a neodymium-loaded liquid scintillator using the same technique used for gadolinium—employing a carboxylate.

To achieve Nd metal loading using carboxylic acid, the process involves dissolving neodymium salt (SNO+ used $NdCl_3$) in an aqueous phase and mixing with a carboxylic acid such as trimethylhexanoic acid. The mixture is subsequently combined with an organic liquid (the liquid scintillator solvent); the organic and aqueous phases separate and neodymium carboxylate transfers efficiently to the organic phase. **Figure 7** shows a sample of Nd-loaded liquid scintillator produced using the carboxylate method along with its UV-Vis absorption spectrum. The Nd-loaded liquid scintillator has a blue color due to absorption bands at longer wavelengths. Any absorption in a liquid scintillator is undesirable; on the other hand the blue color indicates that scintillation light, predominantly blue, can propagate through the liquid.

The R&D into loading neodymium that was carried out at Queen's University also examined nanoparticle suspension as a possible loading technique as well as water-based loading that uses a surfactant to enable non-polar and polar components to be miscible. These two different approaches share some common traits. In stabilizing nanoparticles in a liquid [62] to prevent aggregation, self-assembly and ultimately precipitation, a material (typically a polymer) is layered onto metal inorganic surfaces on a nanoscale. Surface charge properties keep these nanoparticles suspended. Different nanoparticle preparations have different shelf lives. The uniformity of the nanoparticle dispersion would also be an important consideration for this loading approach. In surfactant loading, inverse (or reverse) micelles are formed when a metal is dissolved in water with the surfactant's hydrophilic head groups wrapped around the nanoscale droplet of water. The non-polar ends of the surfactant enable the inverse micelles to be dispersed uniformly in the organic liquid scintillator medium. **Figure 7** also shows (middle vial in the photo) a sample of $NdCl_3$ made miscible in a liquid scintillator using a surfactant.

The development of Nd-loaded liquid scintillator for SNO+ was mature when ultimately it was decided to change the isotope that would be deployed. The motivation for the change was the difficulty to isotopically enrich neodymium. Neodymium does not have gaseous compounds at room temperature. A possibility to enrich ^{150}Nd using AVLIS (atomic vapor laser isotope separation) using an existing but former such facility in France was investigated; however, the cost to reestablish the facility was prohibitive. In order for SNO+ to deploy a significant quantity of double beta decaying isotope without enrichment the focus turned toward tellurium. Additional advantages of ^{130}Te for neutrinoless double beta decay made it very compelling.

The natural abundance of ^{130}Te is 34.1%. Loading natural tellurium into a large liquid scintillator target would enable hundreds of kilograms of ^{130}Te to be deployed in the SNO+ detector. ^{130}Te and ^{136}Xe have very slow $2\nu\beta\beta$ decay rates (the slowest of all double beta decaying isotopes); therefore, a neutrinoless double beta decay signal would have less background from $2\nu\beta\beta$ events. The *Q*-value for the $0\nu\beta\beta$ search with ^{130}Te is 2.529 MeV, very similar to the *Q*-value for ^{136}Xe; thus, many of the low background features of KamLAND-Zen are shared in SNO+ with tellurium. Backgrounds from ^{208}Tl and ^{214}Bi can be identified and rejected with the detection of coincident β/γ signals in the former case, and with the well-known Bi-Po β-α coincidence for the latter. As a result, tellurium and xenon are both very suitable for neutrinoless double beta decay searches employing the loaded liquid scintillator technique.

R&D by SNO+ established two methods for loading tellurium in liquid scintillator. The first method was a surfactant-based approach. Tellurium can be prepared in an aqueous phase and dispersed in a liquid scintillator using a surfactant. The SNO+ liquid scintillator has linear alkylbenzene (LAB) as the primary solvent. A common surfactant is linear alkylbenzene sulfonate; SNO+ used isopropylamine linear alkylbenzene sulfonate as the surfactant to enable tellurium to be suspended in the organic liquid phase.

The method ultimately selected by SNO+ for loading tellurium does not include a surfactant and is different than that for Nd or Gd loading; it is somewhat specific to tellurium although it may also work for other metals with similar chemistry. SNO+ starts with telluric acid, $Te(OH)_6$. When reacted with 1,2-butanediol, a condensation reaction occurs which results in the release of water. Evaporation of the water leaves behind a tellurium-butanediol complex that is soluble in LAB. **Figure 8** illustrates the reaction and an example of the product that is formed. The products of the reaction typically produce more than just the "monomer"; other compounds such as the dimer (that is also illustrated in the figure) are also formed. The synthesis of these compounds is relatively simple; SNO+ completed additional R&D to determine the optimum conditions for carrying out and completing this reaction in order to yield tellurium-loaded liquid scintillator with excellent stability and optical properties. The method for loading tellurium in liquid scintillator yields a very transparent

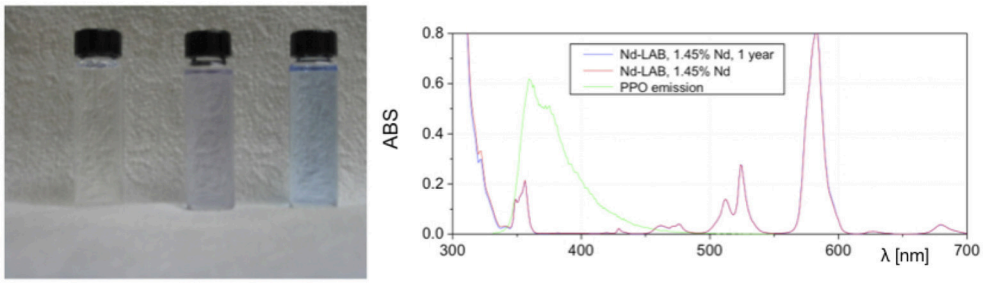

FIGURE 7 | Samples of Nd-loaded liquid scintillator. Left vial: unloaded scintillator; middle vial: Nd-loaded scintillator using a surfactant; right vial: Nd-loaded scintillator made by synthesizing Nd-carboxylate. Right plot: UV-Vis absorption spectrum of Nd-carboxylate loaded in linear alkylbenzene. Absorption in the Nd-loaded samples give the mixture a blue color; overlaid is the emission spectrum from 2,5-diphenyloxazole or PPO.

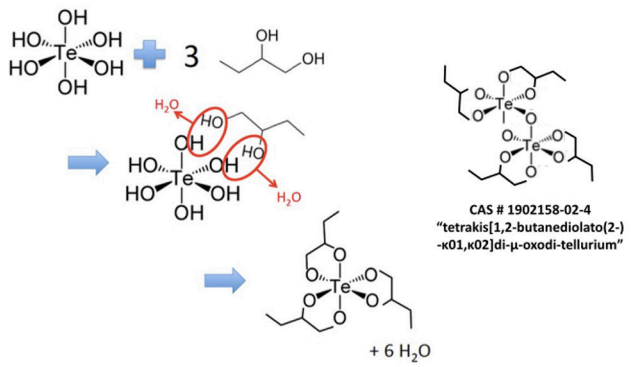

FIGURE 8 | Synthesis of tellurium-butanediol complex which is soluble in linear alkylbenzene for SNO+ Te-loaded liquid scintillator.

mixture with very little absorption and little increased scattering compared to unloaded LAB scintillator. **Figure 9** shows the UV-Vis attenuation spectrum for tellurium-butanediol complex; excellent transparency is maintained in samples of Te-loaded scintillator and optical properties have been found to be stable for more than 2 years.

Tellurium-butanediol will be loaded into SNO+ liquid scintillator at 0.5% Te, by weight. This refers to the weight of tellurium (natural isotopic abundance) and not the weight of the tellurium-butanediol complex. The SNO+ scintillator cocktail has linear alkylbenzene (LAB) as the primary solvent, and contains 2 g/L of the fluor commonly known as PPO (2,5-diphenyloxazole). A secondary wavelength shifter bis-MSB, which is 1,4-bis(2-methylstyryl)benzene, is also added to the cocktail at 20 mg/L concentration. The SNO+ detector will contain 780,000 kilograms of Te-loaded liquid scintillator. At 0.5% Te loading, it will contain 3,900 kg of natural tellurium or 1,330 kg of the isotope ^{130}Te—over 1 ton of isotope will be deployed in SNO+ detector! The fiducial volume in SNO+ is projected to contain about 20% of the total mass.

The SNO+ detector is located where SNO was at 46.475° N, 81.201° W in Vale's Creighton Mine, near Sudbury, Ontario, Canada. The center of the detector is 2039 m below the surface (which is at 309 m above sea level). **Figure 10** is an illustration of the detector configuration.

The main difference between SNO and SNO+ is that heavy water inside the acrylic vessel is replaced with liquid scintillator. Linear alkylbenzene (LAB) scintillator for neutrino physics was developed by the SNO+ group at Queen's University who identified it as having ideal properties for liquid scintillation detectors used for neutrino physics applications: excellent transparency, compatibility with acrylic, safe to use, able to be loaded with metals. LAB has since become a popular choice for use in other neutrino detectors. The consequence of having a liquid with $\rho < 1$ g/cm^3 in the acrylic vessel, surrounded by water, is that the acrylic vessel becomes buoyant in SNO+. A rope net made of low radioactivity Tensylon^{TM} has been installed over the acrylic vessel; the legs of the rope net are attached to anchor plates that are rock-bolted to the bottom of the cavity floor, drilled several meters deep into the rock below. In **Figure 10**, the newly-installed hold-down net can be seen in a photo taken from inside the acrylic vessel.

The geodesic structure in **Figure 10** represents the photomultiplier tube (PMT) support structure, which holds 9,394 PMTs that view the inner volume. The 20-cm diameter Hamamatsu R1408 PMTs are mounted with light-collecting reflectors; the reflectors have aged after years of immersion in pure water during SNO. Their reflectivity and angular response have since been measured *in-situ* and their performance is still very good. Further technical details on the original SNO detector can be found in Boger et al. [63] and also in an upcoming paper on the SNO+ detector.

In addition to the physical changes to the SNO+ detector, additional upgrades to the experiment (since the end of SNO) include upgrading the electronics and DAQ to enable a higher data rate. This accommodates the increased light yield and higher event rates that will be observed with liquid scintillator in the detector. A purification plant for liquid scintillator has been constructed underground (in SNOLAB). Two underground plants for tellurium have also been built—one is a plant for purifying telluric acid and the other is the plant that carries out the tellurium-butanediol synthesis reaction. The former has been installed and commissioning is underway; the latter will be completed in early 2019. The key to the SNO+ double beta

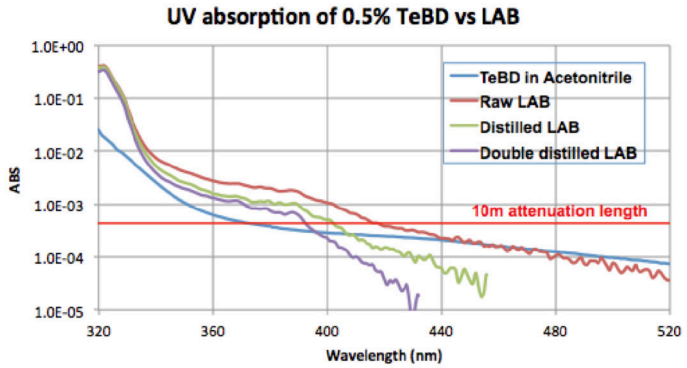

FIGURE 9 | The UV-Vis attenuation (absorption plus scattering) spectrum of synthesized tellurium-butanediol complex compared to that from unloaded linear alkylbenzene (LAB).

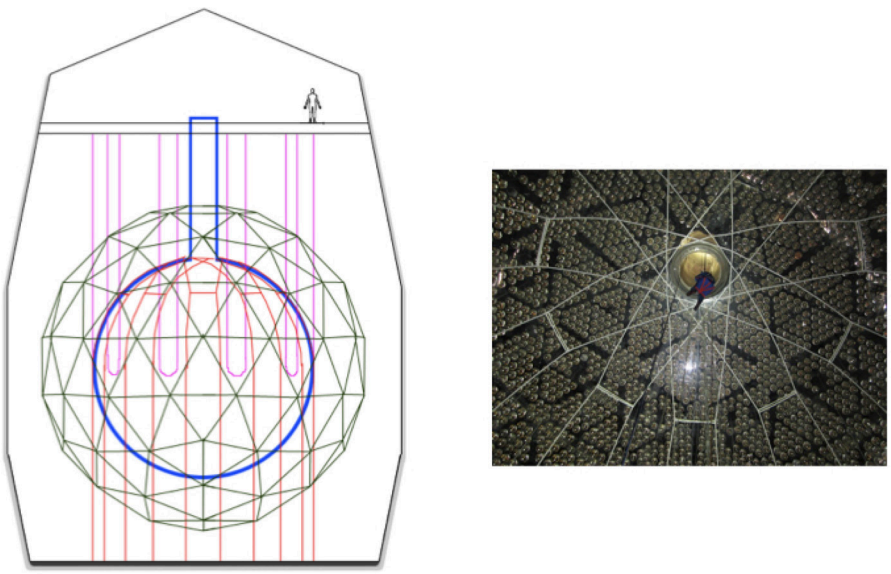

FIGURE 10 | (Left) Schematic of the SNO+ detector (roughly to scale). The 12-m diameter acrylic vessel is in blue. Ropes holding up the vessel are in magenta; the hold-down rope net built for SNO+ is in red. **(Right)** Photo from inside the acrylic vessel, looking up, showing the rope net installed on top of the vessel.

decay search is achieving low backgrounds. The sensitivity of an experiment that is searching for neutrinoless double beta decay boils down to two simple aspects. The first is the quantity of isotope that can be deployed, efficiently, in the detector—this determines the potential signal rate. The second is the amount of background in the double beta decay endpoint region of interest (ROI). Reducing backgrounds in an experiment is a major undertaking. It requires careful selection of materials for radiopurity and it necessitates the purification of materials in the detector (including purification underground to suppress the regrowth of cosmogenic backgrounds). Finally, background rejection techniques are also important to develop as part of an experiment's overall strategy.

Purification of SNO+ telluric acid is carried out using a technique described in Hans et al. [64]. Telluric acid (aqueous) is a weak acid; in the presence of a stronger acid, such as nitric acid, the equilibrium is driven toward precipitating crystals of $Te(OH)_6$. Recrystallization is a purification technique; when telluric acid crystals are induced to precipitate by nitric acid, very pure crystals form. Impurities remain dissolved in the nitric acid that is use to induce recrystallization; the purified crystals are rinsed (with more ultra-pure nitric acid and/or with ultra-pure water). Supplies of nitric acid with ppq levels of U and Th can be obtained. The same techniques used by the company to produce ultra-pure nitric acid have been utilized by SNO+ (in partnership with the company) in order to keep the telluric acid process very clean and ultra-pure. Spike tests with radium and thorium added to telluric acid have demonstrated that purification reduction factors of $>100{,}000$ can be achieved. Similarly, all other components in the SNO+ Te-loaded scintillator cocktail, such as butanediol, have been measured for their intrinsic radiopurity and for the ability

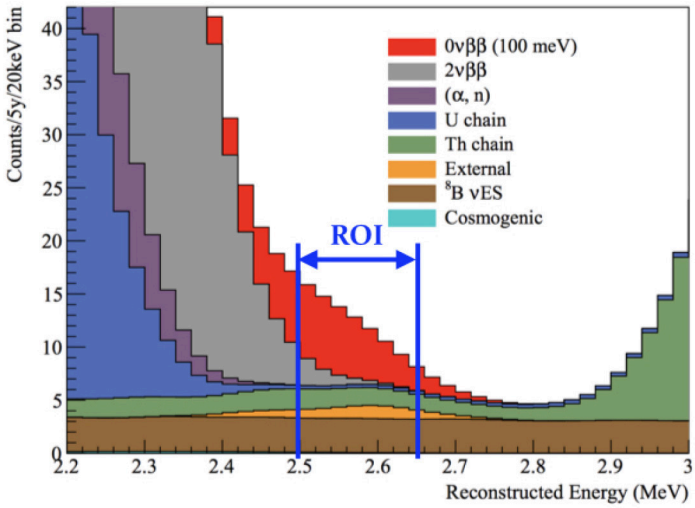

FIGURE 11 | Simulated energy spectrum from 5 years of SNO+ data, assuming backgrounds target levels are achieved.

of purification techniques (such as distillation, in the case of butanediol) to reduce background to ultra-low levels.

With realistic assumptions (and in some cases very conservative ones) about the efficacy of purification, the projected background counting rate in SNO+ with 0.5% Te-loaded scintillator is 12.4 counts/year in the $0\nu\beta\beta$ ROI, between 2.49 and 2.65 MeV. **Figure 11** shows the energy spectrum of events in the fiducial volume with backgrounds at target levels. A hypothetical signal from $0\nu\beta\beta$ with $\langle m_{\beta\beta}\rangle = 100$ meV is also shown in the stacked histogram figure. SNO+ is aiming for background levels in a large liquid scintillator detector to be very low, a remarkable 0.6×10^{-6} counts/keV/kg/year. With this background level, the dominant background in the SNO+ neutrinoless double beta decay search would be ^{8}B solar neutrinos.

At the projected background levels in SNO+, the sensitivity to $0\nu\beta\beta$ for $\langle m_{\beta\beta}\rangle$ reaches down to around 30 meV. This sensitivity would start to probe the region of parameter space suggested by the IH, as shown in **Figure 12**.

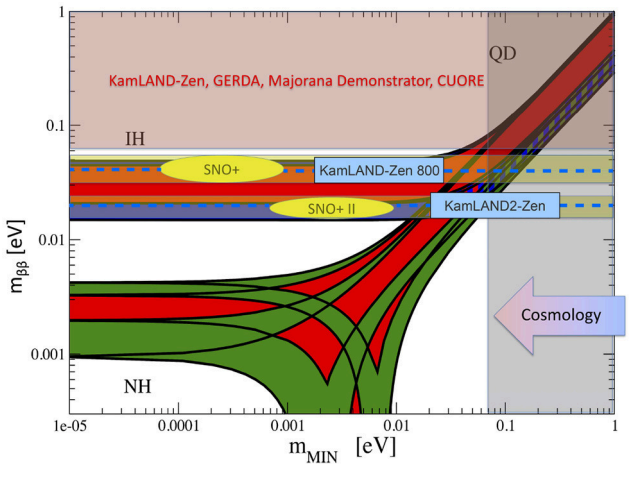

FIGURE 12 | Sensitivity of the KamLAND-Zen 800 experiment increasing the xenon $\beta\beta$ target, the KamLAND2-Zen experiment with an upgraded detector, and the SNO+ experiment with 0.5% Te-loaded liquid scintillator after 5 years of data. If the first phase of SNO+ demonstrates that backgrounds are very low, it would point to a future phase of SNO+ II with 3% Te and improved sensitivity to $\langle m_{\beta\beta}\rangle$. The underlying figure of allowed double beta decay parameter space is adapted from Tanabashi et al. [4] (http://dx.doi.org/10.1103/PhysRevD.98.030001), used with permission.

4. FUTURE PROSPECTS

The KamLAND-Zen collaboration plans to start the upgraded experiment, so called "KamLAND-Zen 800," increasing the xenon $\beta\beta$ decay target to about 750 kg, almost double amount of the previous experiment denoted as "KamLAND-Zen 400." The expected sensitivity on $\langle m_{\beta\beta}\rangle$ is below 50 meV hoping to start the test of the IH region. To accommodate the requirements, a larger and cleaner balloon with less radioactivity was rebuilt with better measures against dust attachment: having workers wear goggles, frequent laundry of cleanroom suits, introducing welding machine, running more neutralizer, covering the nylon film with cover sheets during the welding process, and so on. The balloon installed in 2016 had some LS leakage (before xenon loading) unfortunately due to breaks on the welded lines, so a new balloon was reproduced and installed again in 2018. The data without xenon indicates no LS leakage and ^{232}Th contamination higher than the phase II data in "KamLAND-Zen 400." Prior to xenon loading, the LS needs to be purified by the distillation process to remove ^{232}Th, expected to be completed in 2018.

The next goal is to reach a sensitivity of $\langle m_{\beta\beta}\rangle \sim 20$ meV which covers the IH region. The "KamLAND-Zen 800" sensitivity will be limited by the background mainly from the $2\nu\beta\beta$ decays. The projected sensitivity can be achieved by "KamLAND2-Zen," a detector upgrade plan with better energy resolution against the $2\nu\beta\beta$ background, increasing the light yield by a factor of ~5 with light collecting mirrors (×1.8), new

brighter LS (×1.4), and high quantum efficiency PMTs (×1.9), and with the amount of enriched xenon increased to 1,000 kg or more. The energy resolution is expected to be σ <2.5% at the Q-value of ^{136}Xe $\beta\beta$ decay. The access narrow hole at the top of the detector can be enlarged to accommodate various devices, such as a larger balloon, scintillating crystals containing other $0\nu\beta\beta$ decay nuclei, and a NaI crystal for a dark matter search. Other possible options to improve the sensitivity in KamLAND2-Zen are making the balloon with scintillating film to reject ^{214}Bi-^{214}Po sequential decay backgrounds, and adding an imaging device to reject γ-emitting backgrounds. After the various upgrades, the elastic scattering of solar neutrinos on electrons will be a dominant background source. Its impacts on loaded liquid scintillator experiments are discussed in Ejiri and Zuber [65]. A further ambitious option is "Super-KamLAND-Zen" using a few tens of tons of xenon with higher concentration utilizing high pressure at the bottom of a 20 kton LS detector [34]. It would reach sensitivity to the NH below 10 meV. Another group proposes experiments to enhance sensitivity by measuring directionality in $\beta\beta$ decay and neutrino interactions, based on a technique separating Cherenkov and scintillation light with improved photon detection and timing [66, 67]. Many worldwide R&D efforts for next generation experiments are ongoing.

The SNO+ experiment is about to begin taking data filled with liquid scintillator. Purification of tellurium, underground, and loading of tellurium in the liquid scintillator is scheduled to commence in 2019. SNO+ will soon be a double beta decay experiment utilizing the loaded liquid scintillator technique. If backgrounds are demonstrated to be very low, SNO+ is considering a Phase II deployment of tellurium which would increase the concentration from 0.5 to 3%. The sensitivity of SNO+ II would aim to cover the IH region, as shown in **Figure 12**. High Te loading still retains excellent transparency; on the other hand, higher concentrations of tellurium cause quenching of the intrinsic light yield of the scintillator. Recent R&D by SNO+ has identified mechanisms (in the form of additives to the scintillator cocktail) that combat quenching of scintillation light. With those additives, Te loading of a few percent can be achieved in SNO+ with sufficient light yield. There is also the possibility to increase the light collection by utilizing high quantum efficiency PMTs. If backgrounds from solar neutrinos need to be reduced, options include concentrating the tellurium loading into a smaller volume using a balloon built inside the SNO+ acrylic vessel. Cherenkov light identification may provide directionality information what can also help identify solar neutrino backgrounds, and be used to suppress this background. As the cost of natural tellurium is much less than the cost of enriched isotope, an even larger scale Te-loaded liquid scintillator could be developed with huge amounts of tellurium to enable sensitivity to $0\nu\beta\beta$ effective Majorana neutrino mass values down to the NH region.

5. SUMMARY

Liquid scintillator detectors have played a central role in neutrino research at the MeV energy scale, such as solar, reactor, and geo neutrino observations, developing our understanding of neutrino properties and opening the possibilities of application to astronomical and geoscience research. Meanwhile, new techniques for loading a large amount of nuclei into liquid scintillator have been developed for multiple purposes. It matches the requirements for sensitive searches for $0\nu\beta\beta$ decay. Large liquid scintillator detectors are capable of deploying a large amount of nuclei with different loading techniques. In addition to the high scalability, liquid scintillator has a great advantage in reducing radioactive backgrounds to ultra-low levels. KamLAND-Zen started the measurement of $\beta\beta$ decays by introducing enriched xenon (^{136}Xe) into the liquid scintillator contained in a transparent nylon balloon, and demonstrated the rare decay search in a low background environment. After a drastic background reduction by purification efforts, KamLAND-Zen data showed the non-detection of $0\nu\beta\beta$ decays with about 400 kg xenon, providing a stringent constraint of the effective Majorana neutrino mass $\langle m_{\beta\beta}\rangle < 61 - 165$ meV—a neutrino mass scale close to the inverted hierarchy scale. The search sensitivity will be enhanced by increasing the amount of xenon to double (about 750 kg xenon) and by making a larger and cleaner balloon. SNO+ made a detailed study of loading ^{150}Nd and ^{130}Te into liquid scintillator as double beta decay nuclei. The large natural abundance of ^{130}Te and the ability to load tellurium into the liquid scintillator enables hundreds of kilograms of ^{130}Te to be deployed into the SNO detector converted to be filled with liquid scintillator. The newly developed loading method, specific to tellurium, is effective to produce liquid scintillator with excellent stability and optical properties. The unloaded liquid scintillator detector will be operated soon, and underground plants to produce pure telluric compounds are being finished. The projected sensitivity in SNO+ with 0.5% Te-loaded scintillator is around 30 meV in the effective Majorana neutrino mass. In the future, upgrade plans in KamLAND-Zen and SNO+ aim to reach sensitivities to cover the inverted hierarchy region. Solar neutrinos are a common background source to be overcome for the $0\nu\beta\beta$ search with liquid scintillator detectors. Various new techniques to reduce the solar neutrino background are under development, key to exploring the neutrino mass scale in the normal hierarchy region.

AUTHOR CONTRIBUTIONS

IS has contributed mainly to review the history and current status of double beta decay experiments as well as the current status and prospects of the KamLAND-Zen experiments. MC has contributed mainly to the review of metal loading in liquid scintillator and the SNO+ experiment.

ACKNOWLEDGMENTS

We thank the members of the KamLAND-Zen and SNO+ collaborations, providing information about research activities and recent progress. IS thanks Research Center for Neutrino Science for supporting this work. MC acknowledges support from the Canadian Institute for Advanced Research.

REFERENCES

1. Birks JB. *The Theory and Practice of Scintillation Counting*. Oxford: Pergamon Press (1964).
2. Alimonti G, Anghloher G, Arpesella C, Balata M, Bellini G, Benziger J, et al. Ultra-low background measurements in a large volume underground detector. *Astropart Phys.* (1998) **8**:141–57.
3. Raghavan RS. New approach to the search for neutrinoless double beta decay. *Phys Rev Lett.* (1994) **72**:1411–4. doi: 10.1103/PhysRevLett.72.1411
4. Tanabashi M, Hagiwara K, Hikasa K, Nakamura K, Sumino Y, Takahashi F, et al. Review of particle physics. *Phys Rev D.* (2018) **98**:030001. doi: 10.1103/PhysRevD.98.030001
5. Rodin VA, Faessler A, Šimkovic F, Vogel P. Erratum to: "Assessment of uncertainties in QRPA 0–decay nuclear matrix elements"[Nucl. Phys. A 766 (2006) 107]. *Nucl Phys A.* (2007) **793**:213–5.
6. Menéndez J, Poves A, Caurier E, Nowacki F. Disassembling the nuclear matrix elements of the neutrinoless double beta decay. *Nucl Phys A.* (2009) **818**:139–51. doi: 10.1016/j.nuclphysa.2008.12.005
7. Meija J, Coplen TB, Berglund M, Brand WA, De Bièvre PJ, Gröning M, et al. Isotopic compositions of the elements 2013 (IUPAC Technical Report). *Pure Appl Chem.* (2016) **88**:293–306. doi: 10.1515/pac-2015-0503
8. Wang M, Audi G, Kondev FG, Huang WJ, Naimi S, Xu X. The AME2016 atomic mass evaluation (II). Tables, graphs and references. *Chin Phys C.* (2017) **41**:030003. doi: 10.1088/1674-1137/41/3/030003
9. Arnold R, Augier C, Bakalyarov AM, Baker JD, Barabash AS, Basharina-Freshville A, et al. Measurement of the double-beta decay half-life and search for the neutrinoless double-beta decay of ^{48}Ca with the NEMO-3 detector. *Phys Rev D.* (2016) **93**:112008. doi: 10.1103/PhysRevD.93.112008
10. Agostini M, Allardt M, Bakalyarov AM, Balata M, Barabanov I, Barros N, et al. Results on $\beta\beta$ decay with emission of two neutrinos or Majorons in ^{76}Ge from GERDA Phase I [journal article]. *Eur Phys J C.* (2015) **75**:416. doi: 10.1140/epjc/s10052-015-3627-y
11. Arnold R, Augier C, Barabash AS, Basharina-Freshville A, Blondel S, Blot S, et al. Final results on ^{82}Se double beta decay to the ground state of ^{82}Kr from the NEMO-3 experiment. *Eur Phys J C.* (2018) **78**:821. doi: 10.1140/epjc/s10052-018-6295-x
12. Argyriades J, Arnold R, Augier C, Baker J, Barabash AS, Basharina-Freshville A, et al. Measurement of the two neutrino double beta decay half-life of Zr-96 with the NEMO-3 detector. *Nucl Phys A.* (2010) **847**:168–79. doi: 10.1016/j.nuclphysa.2010.07.009
13. Arnold R, Augier C, Baker J, Barabash A, Broudin G, Brudanin V, et al. First results of the search for neutrinoless double-beta decay with the NEMO 3 detector. *Phys Rev Lett.* (2005) **95**:182302. doi: 10.1103/PhysRevLett.95.182302
14. Barabash AS, Belli P, Bernabei R, Cappella F, Caracciolo V, Cerulli R, et al. Final results of the Aurora experiment to study 2β decay of ^{116}Cd with enriched $^{116}CdWO_4$ crystal scintillators. *Phys Rev D.* (2018) **98**:092007. doi: 10.1103/PhysRevD.98.092007
15. Alduino C, Alfonso K, Artusa DR, Avignone FT, Azzolini O, Banks TI, et al. Measurement of the two-neutrino double-beta decay half-life of ^{130}130Te with the CUORE-0 experiment [journal article]. *Eur Phys J C.* (2017) **77**:13. doi: 10.1140/epjc/s10052-016-4498-6
16. Albert JB, Auger M, Auty DJ, Barbeau PS, Beauchamp E, Beck D, et al. Improved measurement of the 2$\nu\beta\beta$ half-life of ^{136}Xe with the EXO-200 detector. *Phys Rev C.* (2014) **89**:015502. doi: 10.1103/PhysRevC.89.015502
17. Arnold R, Augier C, Baker JD, Barabash AS, Basharina-Freshville A, Blondel S, et al. Measurement of the 2$\nu\beta\beta$ decay half-life of ^{150}Nd and a search for 0$\nu\beta\beta$ decay processes with the full exposure from the NEMO-3 detector. *Phys Rev D.* (2016) **94**:072003. doi: 10.1103/PhysRevD.94.072003
18. Dell'Oro S, Marcocci S, Viel M, Vissani F. Neutrinoless double beta decay: 2015 review. *Adv High Energy Phys.* (2016) **2016**:37. doi: 10.1155/2016/2162659
19. Furry WH. On transition probabilities in double beta-disintegration. *Phys Rev.* (1939) **56**:1184–93. doi: 10.1103/PhysRev.56.1184
20. Fireman EL. Double beta decay. *Phys Rev.* (1948) **74**:1238.
21. Caldwell DO. Double beta decay-present and future. *J Phys G Nucl Part Phys.* (1991) **17**:S137.
22. Aalseth CE, Avignone FT, Brodzinski RL, Cebrian S, Garcia E, Gonzalez D, et al. IGEX ^{76}Ge neutrinoless double-beta decay experiment: prospects for next generation experiments. *Phys Rev D.* (2002) **65**:092007. doi: 10.1103/PhysRevD.65.092007
23. Klapdor-Kleingrothaus HV, Dietz A, Baudis L, Heusser G, Krivosheina IV, Majorovits B, et al. Latest results from the HEIDELBERG-MOSCOW double beta decay experiment. *Eur Phys J A.* (2001) **12**:147–54. doi: 10.1007/s100500170022
24. Klapdor-Kleingrothaus HV, Dietz A, Harney HL, Krivosheina IV. Evidence for neutrinoless double beta decay. *Modern Phys Lett A.* (2001) **16**:2409–20. doi: 10.1142/S0217732301005825
25. Ackerman N, Aharmim B, Auger M, Auty DJ, Barbeau PS, Barry K, et al. Observation of two-neutrino double-beta decay in ^{136}Xe with the EXO-200 detector. *Phys Rev Lett.* (2011) **107**:212501. doi: 10.1103/PhysRevLett.107.212501
26. Gando A, Gando Y, Hanakago H, Ikeda H, Inoue K, Kato R, et al. Measurement of the double-βdecay half-life of ^{136}Xe with the KamLAND-Zen experiment. *Phys Rev C.* (2012) **85**:045504. doi: 10.1103/PhysRevC.85.045504
27. Agostini M, Allardt M, Andreotti E, Bakalyarov AM, Balata M, Barabanov I, et al. Results on neutrinoless double-β decay of ^{76}Ge from phase I of the GERDA experiment. *Phys Rev Lett.* (2013) **111**:122503. doi: 10.1103/PhysRevLett.111.122503
28. Gando A, Gando Y, Hanakago H, Ikeda H, Inoue K, Ishidoshiro K, et al. Limit on neutrinoless $\beta\beta$ decay of ^{136}Xe from the first phase of KamLAND-Zen and comparison with the positive claim in 76Ge. *Phys Rev Lett.* (2013) **110**:062502. doi: 10.1103/PhysRevLett.110.062502
29. Alduino C, Alessandria F, Alfonso K, Andreotti E, Arnaboldi C, Avignone FT, et al. First results from CUORE: a search for lepton number violation via 0$\nu\beta\beta$ decay of ^{130}Te. *Phys Rev Lett.* (2018) **120**:132501. doi: 10.1103/PhysRevLett.120.132501
30. Eguchi K, Enomoto S, Furuno K, Goldman J, Hanada H, Ikeda H, et al. First results from KamLAND: evidence for reactor antineutrino disappearance. *Phys Rev Lett.* (2003) **90**:021802. doi: 10.1103/PhysRevLett.90.021802
31. Abe S, Ebihara T, Enomoto S, Furuno K, Gando Y, Ichimura K, et al. Precision measurement of neutrino oscillation parameters with KamLAND. *Phys Rev Lett.* (2008) **100**:221803. doi: 10.1103/PhysRevLett.100.221803
32. Araki T, McKeown RD, Piquemal F, Mauger C, Vogel P. Experimental investigation of geologically produced antineutrinos with KamLAND. *Nature.* (2005) **436**:499–503. doi: 10.1038/nature03980
33. Gando A, Gando Y, Ichimura K, Ikeda H, Inoue K, Kibe Y, et al. Partial radiogenic heat model for Earth revealed by geoneutrino measurements. *Nat Geosci.* (2011) **4**:647–51. doi: 10.1038/ngeo1205
34. Inoue K. Results from KamLAND-Zen. *Nucl Phys B Proc Sup.* (2013) **235-6**:249–54. doi: 10.1016/j.nuclphysbps.2013.04.018
35. Napolitani P, Schmidt KH, Tassan-Got L, Armbruster P, Enqvist T, Heinz A, et al. Measurement of the complete nuclide production and kinetic energies of the system ^{136}Xe+hydrogen at 1 GeV per nucleon. *Phys Rev C.* (2007) **76**:064609. doi: 10.1103/PhysRevC.76.064609
36. Gando A, Gando Y, Hanakago H, Ikeda H, Inoue K, Kato R, et al. Limits on Majoron-emitting double-β decays of ^{136}Xe in the KamLAND-Zen experiment. *Phys Rev C.* (2012) **86**:021601. doi: 10.1103/PhysRevC.86.021601
37. Bernabei R, Belli P, Cappella F, Cerulli R, Montecchia F, Incicchitti A, et al. Investigation of $\beta\beta$ decay modes in ^{134}Xe and ^{136}Xe. *Phys Lett B.* (2002) **546**:23–8. doi: 10.1016/S0370-2693(02)02671-0
38. Gavriljuk J, Gangapshev A, Kuzminov V, Panasenko S, Ratkevich S. Results of a search for 2β decay of ^{136}Xe with high-pressure copper proportional counters in Baksan Neutrino Observatory. *Phys Nucl.* (2006) **69**:2129–33. doi: 10.1134/S1063778806120180
39. Auger M, Auty DJ, Barbeau PS, Beauchamp E, Belov V, Benitez-Medina C, et al. Search for neutrinoless double-beta decay in ^{136}Xe with EXO-200. *Phys Rev Lett.* (2012) **109**:032505. doi: 10.1103/PhysRevLett.109.032505
40. Rodríguez TR, Martínez-Pinedo G. Energy density functional study of nuclear matrix elements for neutrinoless $\beta\beta$ decay. *Phys Rev Lett.* (2010) **105**:252503. doi: 10.1103/PhysRevLett.105.252503
41. Barea J, Kotila J, Iachello F. Limits on neutrino masses from neutrinoless double-β decay. *Phys Rev Lett.* (2012) **109**:042501. doi: 10.1103/PhysRevLett.109.042501

42. Faessler A, Rodin V, Šimkovic F. Nuclear matrix elements for neutrinoless double-beta decay and double-electron capture. *J Phys G.* (2012) **39**:124006. doi: 10.1088/0954-3899/39/12/124006
43. Klapdor-Kleingrothaus HV, Krivosheina IV. The evidence for the observation of 0nu $\beta\beta$ decay: the identification of 0 events from the full spectra. *Mod Phys Lett A.* (2006) **21**:1547–66. doi: 10.1142/S0217732306020937
44. Doi M, Kotani T, Takasugi E. Double beta decay and Majorana neutrino. *Prog Theor Phys Suppl.* (1985) **83**:481–516. doi: 10.1103/RevModPhys.80.481
45. Gando A, Gando Y, Hachiya T, Hayashi A, Hayashida S, Ikeda H, et al. Search for majorana neutrinos near the inverted mass hierarchy region with KamLAND-Zen. *Phys Rev Lett.* (2016) **117**:082503. doi: 10.1103/PhysRevLett.117.082503
46. Banks TI, Freedman SJ, Wallig J, Ybarrolaza N, Gando A, Gando Y, et al. A compact ultra-clean system for deploying radioactive sources inside the KamLAND detector. *Nucl Instr Methods Phys Res Sect A.* (2015) **769**:88–96. doi: 10.1016/j.nima.2014.09.068
47. Kotila J, Iachello F. Phase-space factors for double-β decay. *Phys Rev C.* (2012) **85**:034316. doi: 10.1103/PhysRevC.85.034316
48. Stoica S, Mirea M. New calculations for phase space factors involved in double-β decay. *Phys Rev C.* (2013) **88**:037303. doi: 10.1103/PhysRevC.88.037303
49. Barea J, Kotila J, Iachello F. $0\nu\beta\beta$ and $2\nu\beta\beta$ nuclear matrix elements in the interacting boson model with isospin restoration. *Phys Rev C.* (2015) **91**:034304. doi: 10.1103/PhysRevC.91.034304
50. Hyvärinen J, Suhonen J. Nuclear matrix elements for $0\nu\beta\beta$ decays with light or heavy Majorana-neutrino exchange. *Phys Rev C.* (2015) **91**:024613. doi: 10.1103/PhysRevC.91.024613
51. Meroni A, Petcov ST, Šimkovic F. Multiple CP non-conserving mechanisms of ()0–decay and nuclei with largely different nuclear matrix elements. *J High Energy Phys.* (2013) **2**:025. doi: 10.1007/JHEP02(2013)025
52. Šimkovic F, Rodin V, Faessler A, Vogel P. $0\nu\beta\beta$ and $2\nu\beta\beta$ nuclear matrix elements, quasiparticle random-phase approximation, and isospin symmetry restoration. *Phys Rev C.* (2013) **87**:045501. doi: 10.1103/PhysRevC.87.045501
53. Mustonen MT, Engel J. Large-scale calculations of the double-β decay of ^{76}Ge, ^{130}Te, ^{136}Xe, and ^{150}Nd in the deformed self-consistent Skyrme quasiparticle random-phase approximation. *Phys Rev C.* (2013) **87**:064302. doi: 10.1103/PhysRevC.87.064302
54. Agostini M, Bakalyarov AM, Balata M, Barabanov I, Baudis L, Bauer C, et al. Improved limit on neutrinoless double-β decay of ^{76}Ge from GERDA phase II. *Phys Rev Lett.* (2018) **120**:132503. doi: 10.1103/PhysRevLett.120.132503
55. Azzolini O, Barrera MT, Beeman JW, Bellini F, Beretta M, Biassoni M, et al. First result on the neutrinoless double-β decay of ^{82}Se with CUPID-0. *Phys Rev Lett.* (2018) **120**:232502. doi: 10.1103/PhysRevLett.120.232502
56. Dell'Oro S, Marcocci S, Vissani F. New expectations and uncertainties on neutrinoless double beta decay. *Phys Rev D.* (2014) **90**:033005. doi: 10.1103/PhysRevD.90.033005
57. Capozzi F, Fogli GL, Lisi E, Marrone A, Montanino D, Palazzo A. Status of three-neutrino oscillation parameters, circa 2013. *Phys Rev D.* (2014) **89**:093018. doi: 10.1103/PhysRevD.89.093018
58. Alfonso K, Artusa DR, Avignone FT, Azzolini O, Balata M, Banks TI, et al. Search for neutrinoless double-beta decay of ^{130}Te with CUORE-0. *Phys Rev Lett.* (2015) **115**:102502. doi: 10.1103/PhysRevLett.115.102502
59. Arnold R, Augier C, Baker JD, Barabash AS, Basharina-Freshville A, Blondel S, et al. Results of the search for neutrinoless double-β decay in ^{100}Mo with the NEMO-3 experiment. *Phys Rev D.* (2015) **92**:072011. doi: 10.1103/PhysRevD.92.072011
60. Barabash AS. Experiment double beta decay: historical review of 75 years of research. *Phys Atom Nucl.* (2011) **74**:603–13. doi: 10.1134/S1063778811030070
61. Ahmad QR, Allen RC, Andersen TC, D Anglin J, Barton JC, Beier EW, et al. Direct evidence for neutrino flavor transformation from neutral-current interactions in the sudbury neutrino observatory. *Phys Rev Lett.* (2002) **89**:011301. doi: 10.1103/PhysRevLett.89.011301
62. Dorris A, Sicard C, Chen MC, McDonald AB, Barrett CJ. Stabilization of neodymium oxide nanoparticles via soft adsorption of charged polymers. *ACS Appl Mater Interfaces.* (2011) **3**:3357–65. doi: 10.1021/am200515q
63. Boger J, Hahn RL, Rowley JK, Carter AL, Hollebone B, Kessler D, et al. The sudbury neutrino observatory. *Nucl Instr Methods Phys Res Sect A.* (2000) **449**:172–207. doi: 10.1016/0168-9002(92)90981-9
64. Hans S, Rosero R, Hu L, Chkvorets O, Chan WT, Guan S, et al. Purification of telluric acid for SNO+ neutrinoless double-beta decay search. *Nucl Instr Methods Phys Res Sect A.* (2015) **795**:132–9. doi: 10.1016/j.nima.2015.05.045
65. Ejiri H, Zuber K. Solar neutrino interactions with liquid scintillators used for double beta-decay experiments. *J Phys G Nucl Part Phys.* (2016) **43**:045201. doi: 10.1088/0954-3899/43/4/045201
66. Aberle C, Elagin A, Frisch HJ, Wetstein M, Winslow L. Measuring directionality in double-beta decay and neutrino interactions with kiloton-scale scintillation detectors. *J Instr.* (2014) **9**:P06012. doi: 10.1088/1748-0221/9/06/P06012
67. Elagin A, Frisch HJ, Naranjo B, Ouellet J, Winslow L, Wongjirad T. Separating double-beta decay events from solar neutrino interactions in a kiloton-scale liquid scintillator detector by fast timing. *Nucl Instr and Meth A.* (2017) **849**:102–11. doi: 10.1016/j.nima.2016.12.033

Conflict of Interest Statement: The authors declare that the research was conducted in the absence of any commercial or financial relationships that could be construed as a potential conflict of interest.